

## Size and Strain Parameters from Peak Profiles: Sense and Nonsense\*

*R. Delhez, Th.H. de Keijser, E. J. Mittemeijer and J. I. Langford<sup>A</sup>*

Laboratory of Metallurgy, Delft University of Technology,  
Rotterdamseweg 137, 2628 AL Delft, The Netherlands.

<sup>A</sup> Department of Physics, University of Birmingham,  
Birmingham, B15 2TT, England.

### *Abstract*

In principle the analysis of positions and shapes of diffraction peak profiles can reveal the imperfect crystalline structure of a sample. The parameters 'size' and 'strain' as obtained from the established Warren–Averbach method need to be used cautiously: in essence the order-independent and order-dependent parts of the line broadening are determined. These require interpretation in terms of structure parameters, for which additional information must often be available. In a case of pure size and strain broadening the order-independent part of the broadening can be interpreted straightforwardly in terms of a size distribution, whereas the order-dependent part cannot readily be related to a specific state of strain. Recent progress in this area is discussed. Non-ideal standard specimens introduce systematic errors. Within the framework of the Warren–Averbach and the single-line Voigt methods, it is shown that this non-ideal situation introduces a constant error and that relative determinations of size and strain are feasible.

Inaccuracy in background determination and the inevitable truncation of a profile at finite range may lead to large errors in line-profile analysis, including the hook effect. Examples show that the error in the strain, normally unappreciated, can be as serious as in the size. It will be argued that a correction for the hook effect needs a reconsideration of the notion 'line profile'; routes for an optimal correction follow from that.

### **1. Introduction**

In principle the analysis of powder diffraction peak profiles can provide a quantitative description of the imperfect crystalline structure of a sample. In practice, however, complications arise because of (i) the unravelling of the contributions of the various types of imperfection that cause changes in the positions and the shape of peak profiles and (ii) the shortcomings of sample preparation and equipment (this paper is restricted to samples for which the kinematical theory of diffraction holds).

In engineering materials many causes for line broadening and/or line shift can be present together: (residual) mechanical stress and gradients thereof, compositional variations, dislocations, finite crystallite size, stacking faults, etc. To quantify each of these causes, an analysis of a variety of independent diffraction data is required in general. For example, shape parameters of more than one profile are utilised, or data from line positions are combined with data obtained from line shapes. Incidentally, description of the microstructure may be restricted to an interpretation of only the

\* Paper presented at the International Symposium on X-ray Powder Diffractometry, held at Fremantle, Australia, 20–23 August 1987.

positions of profiles e.g. measured from the specimen tilted over different angles about an  $\omega$  or a  $\psi$  axis; an example is given in Section 5*a*. Such detailed analyses are only feasible if one can indicate beforehand the types of imperfection that play a part.

In the absence of *a priori* knowledge about the types of imperfection present, the well-established Warren–Averbach method for line-broadening analysis can be applied to characterise the imperfect crystalline structure of a sample. The method needs (minimally) two peak profiles. In fact, apparently order-independent and order-dependent parts of the broadening are separated. These parts, traditionally ascribed to size and microstrain, contain contributions from various kinds of imperfections present and therefore it is preferable to speak about effective size and effective microstrain and to be cautious in the interpretation of these (see Section 2).

In size/strain determination the peak profile shape has to be analysed and then one is inclined to ignore the information contained in the position of the peak profiles, although this information is obtainable without any additional experimental work! Conversely, in stress determination by means of peak position analysis (the  $\sin^2\psi$  method) one tends to ignore the line broadening. An example will be given where the benefits of both position and shape analysis become evident (Section 5*b*).

Peak profile positions and shapes are affected by the shortcomings of powder diffraction equipment. Extensive theoretical studies about this have been made (Wilson 1963; Klug and Alexander 1974). In practice, corrections based on these studies are frustrated since (often) accurate knowledge is lacking about the values of the parameters characterising the shortcomings of the instrument. Therefore, one prefers to rely on reference specimens. However, reference specimens are seldom perfect. With respect to this, attention will be drawn to relative determinations of peak positions, effective size and effective strain values (Section 3).

Inaccurate determination of background and truncation of a profile, owing to the unavoidable limitation of the measurement range (overlap of profiles), lead to large errors in values determined for the effective size and effective microstrain. It will be argued that a correction for truncation needs a reconsideration of the notion ‘line profile’. Approaches to the correction for truncation will be discussed in Section 4.

## 2. The Notions ‘Size’ and ‘Microstrain’

The Warren–Averbach method (1950, 1969) for the analysis of diffraction line broadening can be executed on the basis of

$$A(L, d) = A^S(L) A^D(L, d) = A^S(L) \{1 - 2\pi^2 L^2 \langle e^2(L) \rangle / d^2\}, \quad (1)$$

where  $A$  denotes the normalised,  $A(0, d) = 1$ , cosine Fourier coefficient of the broadened profile (instrumental broadening removed),  $L$  is a (correlation) distance in the crystals measured in a direction perpendicular to the reflecting lattice planes,  $d$  is the (average) interplanar spacing corresponding to the (peak position or the centroid of the) profile examined,  $A^S$  is the cosine Fourier coefficient containing the information about size (see however Section 2*a*),  $A^D$  is the cosine Fourier coefficient containing the information about microstrain (see however Section 2*a*), and  $\langle e^2(L) \rangle$  is the mean squared strain averaged over the  $L$  value regarded, with the angle brackets indicating an average over all intervals of length  $L$  occurring in the sample. Further,  $e(L)$  is not a strain as defined usually in physics, but corresponds to the components

(along the normal to the diffracting planes) of the displacement vectors at positions a distance  $L$  apart.

From the first and second 'derivatives' (see Section 4) of  $A^S(L)$  with respect to  $L$  one obtains the average column length (equal to the area-weighted crystallite size) and the column-length distribution (particle size distribution) respectively; information about size is obtained only in a direction perpendicular to the lattice planes considered.

The terms in braces in equation (1) stem from a series expansion and only hold for small values of  $L$ . Originally a logarithm figured in equation (1), but it was shown (Delhez and Mittemeijer 1976) that the above form of equation (1) is the less prejudiced and is therefore to be preferred. For different orders of reflection by the same lattice planes, the  $A^S(L)$  and  $\langle e^2(L) \rangle$  are the same and can therefore be obtained from plots of  $A(L, d)$  versus  $d^{-2}$  for each  $L$  desired. For an overview about details of the theory, experimental procedures and data evaluation the reader is referred to Delhez *et al.* (1980, 1982).

#### (a) Conceptual Problems

For the case of pure size broadening, the Fourier coefficients of a line profile can be straightforwardly interpreted in the sense as given above for  $A^S$  (Bertaut 1950). Then the second derivative of  $A^S$  with respect to  $L$ , which is a measure for the fraction of columns of size  $L$ , can never be negative. If this occurs nevertheless, errors in the experiment or in the data evaluation must be the cause. For example, in the case where the background of a line profile is estimated too high and the profile tails are truncated (because of overlapping of profiles) a 'hook effect' will occur (Delhez *et al.* 1982): the second derivative of the Fourier coefficient curve near  $L = 0$  is then negative.

In general, however, if size and strain broadening occur simultaneously, the presence of a hook effect in  $A(L, d)$  does not need to be an indication of erroneous experimental data. The microstrain itself (cf. equation 1) as well as instrumental aberrations may produce a hook effect in the Fourier coefficient curve of experimental profiles. The only hook effect that is suspect is that in  $A^S(L)$  and therefore all hook-effect corrections applied to Fourier coefficients other than  $A^S(L)$  are premature and spurious.

Even a hook effect in the  $A^S(L)$  curve needs due consideration. Equation (1) was originally developed for the case of (homogeneously) cold-worked metals. In applying the Warren-Averbach method, whatever the nature of the imperfections in the crystalline structure might be, peculiar results may be obtained, possibly also a hook effect in the  $A^S(L)$  curve [e.g. for crystals containing small angle boundaries (Wilkens 1979)]. In such cases, having accepted that the order-dependence of the broadening obeys (1), one has to realise that in fact, from a plot of  $A(L, d)$  versus  $d^{-2}$ , an order-independent part denoted by  $A^S(L)$  and an order-dependent part of the broadening represented by  $\langle e^2(L) \rangle$  is determined. Such  $A^S(L)$  and  $\langle e^2(L) \rangle$  values might be very helpful in comparative studies of (changes in) the imperfect crystalline structure of materials; for absolute, physically meaningful results a further interpretation based on additional information is required. In the analysis of complicated crystalline structures computer simulation of line profiles can be an indispensable tool (Turunen 1976).

In the Warren-Averbach theory the general form of equation (1) is

$$A(L, d) + i B(L, d) = A^S(L) \{ A^D(L, d) + i B^D(L, d) \}, \quad (2)$$

where  $B$  denotes the sine Fourier coefficient. The size Fourier coefficients is always real, i.e.  $B^S(L) = 0$ . In the application of the Warren–Averbach method, it might be helpful to inspect the sine coefficients also and to check if the order-independent part (for small  $L$ ) is indeed zero within the experimental error. If the sine coefficients are not analysed nonetheless, then a Warren–Averbach type analysis of the modulus of the Fourier coefficients rather than of the cosine coefficient is preferred, since then problems arising from an improper choice of origin are avoided (Delhez *et al.* 1982).

At first sight, from the parameters obtained by a Warren–Averbach analysis of any sample, the average crystallite size seems to have a clear meaning in contrast to the mean squared strain  $\langle e^2(L) \rangle$ . In fact the meaning of both parameters and the values obtained for them is unclear. The Warren–Averbach theory is based on the assumption of small domains diffracting incoherently with respect to each other. Obviously, the theory holds for a specimen consisting of one domain. In imperfect crystalline structures, however, abrupt domain boundaries seldom occur. As a consequence the  $A^S(L)$  and  $\langle e^2(L) \rangle$  for different orders of reflection may differ and this affects the basis for the size–strain separation. At the moment, however, for general purposes, there is no real alternative to the Warren–Averbach analysis method.

### (b) Interpretation of Microstrain Parameters

The full characterisation of an imperfect crystalline structure is very complicated. However, a highly detailed description is not needed and even unwanted since in the physics and chemistry of the imperfect crystalline solid state the models used are still rather primitive and require only a few input parameters. In such models an average crystallite size and possibly a variance of the size distribution will serve, but averaged squared strain values for a number of correlation distances are not manageable. Especially not since the meaning of the  $\langle e^2(L) \rangle$  versus  $L$  curve and the  $\langle e^2(L) \rangle$  values themselves is too vague: there is too much averaging involved.

Theoretically, strain distributions for each  $L$  value can be extracted from diffraction experiments, but a very large number of profiles is needed. To avoid the problem, sometimes a seemingly sensible mean squared strain value, out of the  $\langle e^2(L) \rangle$  distribution, is given as a characteristic for the material analysed, e.g. for  $L$  equal to the average crystallite size or half of it or even, quite arbitrarily, for  $L$  equal to 50 Å. Also, attempts have been made to find an analytical description of the  $\langle e^2(L) \rangle$  versus  $L$  curve (Rothman and Cohen 1969; Adler and Houska 1979). A function of the type  $\langle e^2(L) \rangle = CL^{-r}$ , where  $C$  and  $r$  ( $>0$ ) are adaptable parameters, seems to fit for large  $L$  in a number of practical cases, but no general theoretical basis supporting this exists. In any case, by the last method more information is transmitted than by just presenting a single  $\langle e^2(L) \rangle$  value.

Of all  $\langle e^2(L) \rangle$  values the  $\langle e^2(0) \rangle$  value is the most interesting since it concerns a local strain (as normally used in physics) and it can be related to, for example, the energy stored in the imperfect crystalline structure. However,  $\langle e^2(0) \rangle$  cannot be determined directly by the Warren–Averbach method and also a simple graphical extrapolation to  $L = 0$  of the  $\langle e^2(L) \rangle$  versus  $L$  curve does not result in trustworthy values since, near  $L = 0$ , the  $\langle e^2(L) \rangle$  versus  $L$  curve usually decreases sharply with increasing  $L$  (the above-mentioned function  $CL^{-r}$  with  $r > 0$  fails of course near  $L = 0$ ).

Recently a method for the interpretation of Warren–Averbach mean squared strain curves was presented (Turunen *et al.* 1983). It can be shown that

$$\langle e^2(L) \rangle = \sum_{n=0}^{\infty} C_{2n} L^{2n}, \quad (3)$$

where the first three coefficients have the expressions

$$C_0 = \langle e(0)^2 \rangle, \quad C_2 = \langle e(0) e^{(ii)}(0) \rangle / 12,$$

$$C_4 = \langle e(0) e^{(iv)}(0) \rangle / 960 + \langle e^{(ii)}(0)^2 \rangle / 576,$$

with  $e^{(ii)}$  and  $e^{(iv)}$  as the second and fourth derivatives with respect to distance in the crystal perpendicular to the diffracting planes. Averages of products of  $e(0)$  and its derivatives are not more tractable in current possible models for imperfect crystalline material than average strain values as a function of the correlation distance  $L$  (see discussion at the start of Section 2*b*). But, as a consequence of the assumption that the division of the crystals into columns is random with respect to strain, it can be deduced that

$$C_{2n} = \frac{2(-1)^n}{(2n+2)!} \langle e^{(n)}(0)^2 \rangle. \quad (4)$$

Fitting of equation (3) to the experimentally determined  $\langle e^2(L) \rangle$  versus  $L$  curve yields the coefficients  $C_{2n}$  from which, by use of equation (4), the squared *local* strain and the squared *local* strain derivatives with respect to distance can be obtained separately.

The method was applied in a study of the recovery in deformed aluminium. It was found that by annealing for a constant time at different temperatures up to 574 K:

- (i) the halfwidths of the peak profiles obtained with Co K $\alpha$  radiation changed only little with increasing temperature: from  $0.113^\circ 2\theta$  to  $0.102^\circ 2\theta$  for (200) and from  $0.238^\circ 2\theta$  to  $0.165^\circ 2\theta$  for (400), whereas the halfwidths of the instrumental profiles were  $0.091^\circ 2\theta$  for (200) and  $0.136^\circ 2\theta$  for (400);
- (ii) the mean squared local strain decreased only slightly with increasing temperature, indicating a small decrease in dislocation density; but
- (iii) the mean squared local derivatives showed a (relatively strong) increase with increasing temperature, followed by a decrease, for which an explanation was given in terms of changes in the dislocation arrangements in the specimen.

The method appears rather sensitive as no clear differences in the dislocation structure could be resolved in the electron microscope after the different annealing treatments. A routine application of the method is hindered by the very accurate data accumulation required.

### 3. Relative Determinations of Size and Strain

Powder diffraction equipment is never ideal; peak profile positions and shapes are affected by the inherent aberrations from the ideal construction. To compensate, reference specimens are used. Reference specimens used in the determination of size and strain on an absolute scale must satisfy a number of severe requirements, amongst others:

- (i) the material should be ideally crystallised;
- (ii) the grain size should be large enough to avoid significant size broadening and should be small enough to avoid bad crystal statistics;
- (iii) the transparency for the radiation employed should be the same as for the sample analysed; and
- (iv) the positions of the reference peak profiles should be the same as for the peak profiles analysed.

Even in the case where the reference material is of the same chemical composition as the material analysed, problems may arise if the sample is subjected to mechanical stresses. Then the positions of the profiles recorded from the reference and from the sample analysed do not coincide. As the instrumental aberrations are angle dependent, the reference profiles are not a fully correct representation of the instrumental broadening corresponding to the positions of the profiles investigated. Corrections for the effects of non-ideal reference profiles are easily accomplished (to a great part) and should not be omitted since rather serious errors can occur (Keijser and Mittemeijer 1978, 1980).

In many cases the imperfect crystalline structure need not be characterised (e.g. in terms of size and microstrain) on an absolute scale. Very often it suffices to trace changes in the imperfect crystalline structure as induced by some treatment or an alteration in the preparation conditions of the material. Then an analysis on a relative scale, with reference to a defined starting condition of the specimen, should be preferred. This avoids uncertainties about the quality of the 'ideal' reference specimen and, even more important, ambiguities in the interpretation of the line broadening (see Section 2) may be reduced.

For the multiple-line Warren-Averbach method it was shown, without any further assumptions (Zemitis *et al.* 1972; Keijser and Mittemeijer 1978), that sound relative determinations of size and strain are possible on the basis of the following equations:

$$\langle D \rangle_{a,m}^{-1} = \langle D \rangle_a^{-1} - \langle D \rangle_{a,0}^{-1}, \quad \langle e^2(L) \rangle_m = \langle e^2(L) \rangle - \langle e^2(L) \rangle_0, \quad (5, 6)$$

where  $\langle D \rangle_{a,m}$  denotes the (area-weighted) average crystallite size as determined relative to a reference sample containing structural defects,  $\langle D \rangle_a$  denotes the absolute average crystallite size in the sample and  $\langle D \rangle_{a,0}$  denotes the absolute average crystallite size in the reference sample employed; an analogous notation is used for the microstrain  $\langle e^2(L) \rangle$ . Clearly, changes in  $\langle D \rangle_a$  and  $\langle e^2(L) \rangle$  are identical to changes in  $\langle D \rangle_{a,m}$  and  $\langle e^2(L) \rangle_m$ .

Also, for the single-line Voigt analysis method (Keijser *et al.* 1982) sound relative determinations of size and microstrain parameters are possible, as is shown below.

In the single-line Voigt method all profiles are described by Voigt functions, which are convolutions of Cauchy and Gaussian functions. From the full width at half maximum  $2w$  and the integral breadth  $\beta$  of a Voigt profile, one can obtain straight away the integral breadths of the constituting Cauchy and Gaussian profiles (in the following the subscripts C and G indicate Cauchy and Gaussian components). The integral breadths of the Cauchy and Gaussian components of the pure, only structurally broadened profile follow from

$$\beta_C^f = \beta_C^h - \beta_{C,0}^g, \quad (\beta_G^f)^2 = (\beta_G^h)^2 - (\beta_{G,0}^g)^2, \quad (7, 8)$$

where the subscript f refers to a pure, only structurally broadened profile, h to a measured profile of the sample investigated, and g to a profile corresponding to a hypothetical ideal reference sample (subscript 0).

When a reference sample is employed with an imperfect crystalline structure, i.e. for which the crystallite size is not infinitely large and/or the microstrain is not zero, one obtains

$$\beta_{C,m}^f = \beta_C^h - \beta_{C,m}^g, \quad (\beta_{G,m}^f)^2 = (\beta_G^h)^2 - (\beta_{G,m}^g)^2, \quad (9, 10)$$

where the subscript m marks data from measurements in which a non-ideal reference sample is involved. Introducing the symbols  $\beta_{C,0}^f = \beta_{C,m}^g - \beta_{C,0}^g$  and  $\beta_{G,0}^f = \{(\beta_{G,m}^g)^2 - (\beta_{G,0}^g)^2\}^{1/2}$ , representing the structural broadening by the reference sample, equations (9) and (10) can be rewritten using (7) and (8):

$$\beta_{C,m}^f = \beta_C^f + \beta_{C,0}^g - \beta_{C,0}^f - \beta_{C,0}^g = \beta_C^f - \beta_{C,0}^f, \quad (11)$$

$$(\beta_{G,m}^f)^2 = (\beta_G^f)^2 + (\beta_{G,0}^g)^2 - (\beta_{G,0}^f)^2 - (\beta_{G,0}^g)^2 = (\beta_G^f)^2 - (\beta_{G,0}^f)^2. \quad (12)$$

In the single-line Voigt method it is assumed that the Cauchy component of the f profile is solely due to finite crystallite size and that the Gaussian component of the f profile is solely due to microstrain:

$$\langle D \rangle_v = \frac{\lambda \cos \theta}{\beta_C^f}, \quad \tilde{\epsilon} = \frac{\beta_G^f}{4 \tan \theta}, \quad (13, 14)$$

where  $\lambda$  is the wavelength of the radiation employed,  $\theta$  is the Bragg angle, the subscript v denotes a volume-weighted average and  $\tilde{\epsilon}$  is a measure for the microstrain. These size and strain parameters differ from those employed in the Warren–Averbach method (cf. Delhez *et al.* 1982; Langford *et al.* 1988, present issue p. 173). From equations (11)–(14) it follows that

$$\langle D \rangle_{v,m}^{-1} = \langle D \rangle_v^{-1} - \langle D \rangle_{v,0}^{-1}, \quad \tilde{\epsilon}_m^2 = \tilde{\epsilon}^2 - \tilde{\epsilon}_0^2. \quad (15, 16)$$

As with equations (5) and (6), changes in  $\langle D \rangle_v$  and  $\tilde{\epsilon}^2$  are identical to changes in  $\langle D \rangle_{v,m}$  and  $\tilde{\epsilon}_m^2$ .

Of course, single-line methods are dubious in many respects, but very often no alternative is possible. However, the drawbacks of a single-line method are far less serious in relative determinations than in determinations on an absolute scale. This holds in particular if changes occur in either size or strain.

#### 4. Effects of and Correction for Truncation

In powder diffraction the  $2\theta$  range over which a line profile can be measured is limited by the presence of neighbouring reflections. This leads to a (vertical) truncation of profile tails and an incorrect estimation of background (usually too high; horizontal truncation). Thereby intensity, and thus information, is 'lost'. The Fourier coefficients of a line profile are affected by truncation, amongst others a hook effect is introduced (see Section 2). The zeroth Fourier coefficient, which is equal to the average intensity in the range of measurement, directly reflects the loss of intensity: the percentage decrease in intensity is equal to the percentage decrease in the zeroth

Fourier coefficient. The adverse effects of truncation in line profile analysis have been discussed frequently in the literature.

The large errors in the effective crystallite size introduced by truncation are well known. A false procedure in size determination must be indicated. Recognising that truncation in particular affects the zeroth discrete\* Fourier transform value, the initial slope and thus the crystallite size has been estimated from the first and second discrete Fourier transform values. However, by the inherent curvature of the transform as a result of a size distribution, the crystallite size will be severely overestimated, even if the discrete Fourier transform values have been corrected for truncation effects (see Fig. 1; for a better procedure see Delhez *et al.* 1986). There is a tendency to overlook the very serious effects of truncation in the determination of effective microstrains.

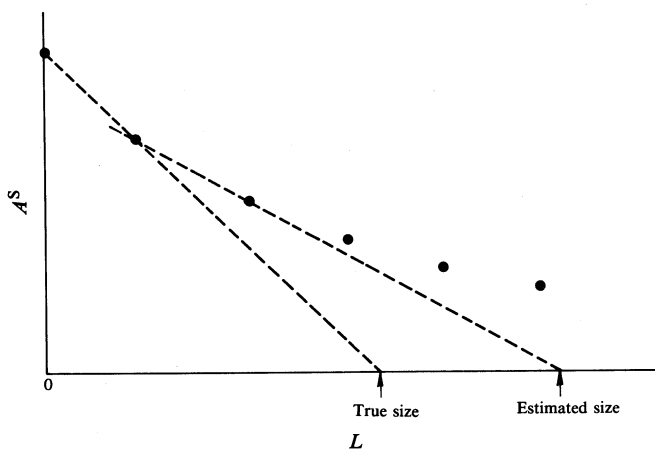


Fig. 1. Discrete Fourier transform values  $A^S$  for the only size broadened profile versus the distance  $L$  perpendicular to the reflecting planes. The true size is obtained from the zeroth and first  $A^S$  values. An erroneous estimated size follows from the first and second  $A^S$  values.

For a Warren–Averbach analysis using two orders of reflection, the error in the microstrains only due to the truncation-induced decreases in the zeroth Fourier coefficients of the different orders of reflection can be estimated. From equation (1) it follows that

$$\langle e^2(L) \rangle_m = \frac{d_1^2 d_2^2}{d_1^2 - d_2^2} \frac{1}{2\pi^2 L^2} \left( \frac{A(L, d_1)_m}{A(0, d_1)_m} - \frac{A(L, d_2)_m}{A(0, d_2)_m} \right) / A^S(L)_m,$$

where  $d_1$  and  $d_2$  are the lattice spacings corresponding to the two orders of reflection studied and the subscript  $m$  is for data obtained from the measurements without any correction for truncation. If corrected values for the zeroth Fourier coefficients are used, i.e.  $A(0, d)_c = A(0, d)_m + \Delta A(0, d)$ , one obtains a corrected value for the mean squared strain,  $\langle e^2(L) \rangle_c$ , by replacing  $A(0, d)_m$  by  $A(0, d)_c$  and  $A^S(L)_m$  by  $A^S(L)_c$  in the expression for  $\langle e^2(L) \rangle_m$ . With  $d_1 = 2d_2$  and for small values of  $L$ , where

\* The Fourier transform of a measured profile can only be obtained in a discrete manner (sampling in Fourier space). For the use of Fourier transform versus Fourier coefficients in line profile analysis, see further in this section.

it is permissible to make the approximations  $A(L) \approx A^S(L)_m \approx A^S(L)_c \approx 1$  and  $\{1 + \Delta A(0, d)_m / A(0, d)_m\}^{-1} = 1 - \Delta A(0, d) / A(0, d)$ , it immediately follows that

$$\langle e^2(L) \rangle_c - \langle e^2(L) \rangle_m = \frac{1}{6\pi^2} \left( \frac{d_1}{L} \right)^2 \left( \frac{\Delta A(0, d_2)}{A(0, d_2)} - \frac{\Delta A(0, d_1)}{A(0, d_1)} \right). \quad (17)$$

Equation (17) is graphically displayed in Fig. 2.

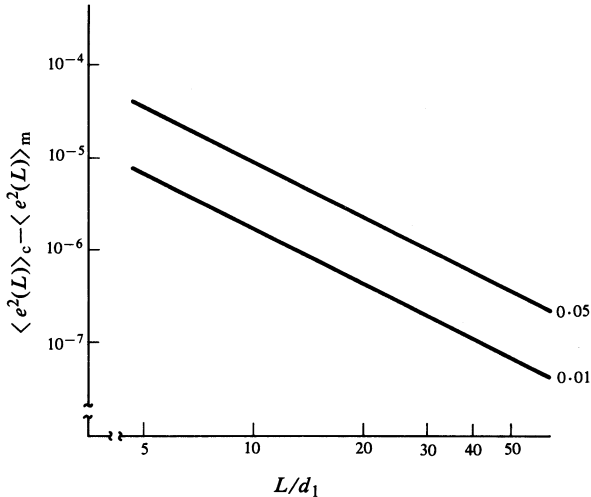


Fig. 2. Error in the Warren-Averbach microstrains due to the truncation-induced errors in the zeroth Fourier coefficients of two different orders of reflection (cf. equation 17) for  $\Delta A(0, d_2) / A(0, d_2) - \Delta A(0, d_1) / A(0, d_1)$  equal to 0.05 and 0.01 for the case  $d_1 = 2d_2$ .

The values of  $\Delta A(0, d_2)$  and  $\Delta A(0, d_1)$  are positive and thus some compensation of errors occurs. In common powder diffraction practice, the separation on a  $d^{-1}$  scale between high order reflections is less than between low order reflections and also the peak-to-background ratio is less favourable for high order than for low order reflections. So one may expect  $\Delta A(0, d_2) > \Delta A(0, d_1)$  and thus too low values for the microstrain. As can be seen from Fig. 2 very large errors can occur (usually  $\langle e^2(L) \rangle$  less than  $10^{-4}$ )!

A correction for the effects of vertical and horizontal truncation requires a mathematical description of the unmeasured parts of the profile tails. This description depends critically on the type(s) of imperfection(s) present in the material to investigate and is generally not known in advance. Therefore, a correction for truncation has to be based on a reasonable expectation about the behaviour of the diffracted intensity beyond the limits of the measured range. Also, an iterative procedure may be devised in which the tail-shape function for the next step follows from the foregoing step. Iterative procedures, in which at every turn the same tail function, but with adjusted values for its parameters, is used, may be dangerous, since the results obtained are then fully confined to the shackles of the function chosen.

Sometimes mathematical functions are fitted to all intensities observed in the range

of measurements, e.g. with full pattern profile fitting. In such procedures the problem of truncation (or more appropriate in this context the intensity/shape-information loss) is seemingly avoided or is very difficult to establish. In a few of such cases the absence of a hook effect was considered to prove the validity of the shape function and/or the procedure employed. This is false logic, since then the presence or absence of a hook effect is fully determined by the mathematical properties of the fitting function employed, no matter how well the function fits and how small or large the extent of the 'truncation'. The absence of a hook effect may even hint at an incorrect fitting function, since with microstrain and with instrumental aberrations there can be an inherent negative curvature of the Fourier transform  $A(L, d)$  at small  $L$  (see Section 2).

A correction for truncation needs a careful consideration of the notion 'line profile' in order to find out the most reasonable mathematical function(s) for the profile tails lost (Delhez *et al.* 1986). Traditional applications of the kinematical diffraction theory provide a relation between the total intensity distribution in reciprocal space and the structural parameters [e.g. size and strain in the Warren–Averbach theory (Warren 1969)]. This total intensity distribution peaks at or near reciprocal lattice points. Warren–Averbach analysis then implies a Fourier series development of parts of this total intensity distribution within chosen intervals of the type  $[l - \frac{1}{2}, l + \frac{1}{2}]$  ( $l$  indicates the node considered in reciprocal space).

For pure size broadening, it can be shown that the total intensity distribution is described also exactly by an infinite sum of 'component' line profiles. Each component line profile is confined to a single reciprocal lattice point and extends from  $-\infty$  to  $+\infty$ : component line profiles always overlap. Analyses of component line profiles imply Fourier transformations instead of Fourier series.

For details about the theory and preliminary suggestions for truncation correction procedures the reader is referred to Delhez *et al.* (1986).

## 5. Examples of Detailed Microstructural Information obtainable from Peak Profile Analysis

In the literature, many examples of straightforward analysis of profile shape for microstructural characterisation are given (e.g. Klug and Alexander 1974). In most cases the information present in the line profiles measured is not fully extracted. To illustrate this and also because of remarks in Sections 2 and 3, two case studies are described, which show that much microstructural information can be obtained from line position analysis also (Section 5*a*), and that in general an analysis of both line position and line shape should be performed in order to arrive at a more complete picture of the microstructure investigated (Section 5*b*).

### *(a) Peak Position Analysis; Determination of Composition, Mechanical Stress and Stacking Fault Density Simultaneously*

CuCr multilayers on a Cu substrate were investigated as evaporated and after subsequent laser irradiation (details are given in Westendorp *et al.* 1986). For the Cu-rich phase the (macro)stresses, the amount of Cr in solid solution and the stacking-fault densities were determined on the basis of peak profile positions, from which (apparent) lattice spacings were calculated.

The penetration depth of the X-rays was considerably larger than the 0.5  $\mu\text{m}$  thickness of the multilayer, so average properties of the multilayer are obtained from

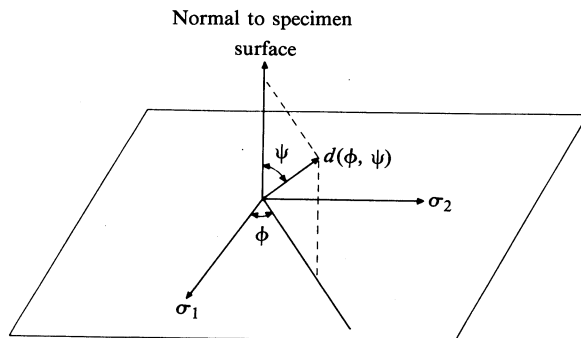


Fig. 3. Principal stresses  $\sigma_1$  and  $\sigma_2$  and the angles  $\phi$  and  $\psi$ .

the diffraction analysis. In view of the geometry of the multilayer/substrate system and the requirement of equilibrating forces, it is justified to adopt for both the as evaporated and the laser-irradiated multilayer an average state of stress which is biaxial and which has the principal stresses  $\sigma_1$  and  $\sigma_2$  parallel to the specimen surface (this is also sustained by the results obtained). The lattice spacing  $d(\phi, \psi)$  of the  $(hkl)$  planes measured in the direction  $(\phi, \psi)$  (see Fig. 3) is then related to the stress-free spacing  $d_0$  by

$$\frac{d(\phi, \psi) - d_0}{d_0} = S_1(hkl)(\sigma_1 + \sigma_2) + \frac{1}{2}S_2(hkl)(\sigma_1 \cos^2 \phi + \sigma_2 \sin^2 \phi) \sin^2 \psi, \quad (18)$$

where  $S_1(hkl)$  and  $\frac{1}{2}S_2(hkl)$  are the so-called X-ray elastic constants (Cohen *et al.* 1980; Hauk and Macherauch 1983). Since  $d_0$  and  $d(\phi, \psi=0)$  differ very little, in this analysis they can be interchanged in the denominator on the left-hand side of (18). For the specimens investigated it was experimentally shown that  $d(\phi, \psi)$  did not depend on  $\phi$ , i.e.

$$\sigma_1 = \sigma_2 \equiv \sigma_{\parallel}. \quad (19)$$

Then (18) can be rewritten as

$$\frac{d(\psi) - d_0}{d_0} - 2S_1(hkl)\sigma_{\parallel} = \frac{d(\psi) - d(\psi=0)}{d(\psi=0)} = \frac{1}{2}S_2(hkl)\sigma_{\parallel} \sin^2 \psi. \quad (20)$$

By measuring, as a function of  $\psi$ , the lattice spacing of the planes  $(hkl)$  for which  $S_1(hkl)$  and  $\frac{1}{2}S_2(hkl)$  are known, one can determine the stress  $\sigma_{\parallel}$  from the slope of the straight line through the data points in a plot of  $d(\psi)$  versus  $\sin^2 \psi$  (cf. equation 20) and from this, the term  $2S_1(hkl)\sigma_{\parallel}$ .

In general the lattice spacing of a material changes when a second component is dissolved:

$$\frac{d_c - d_r}{d_r} = f(c), \quad (21)$$

where  $d_c$  is the strain-free spacing of the material with an atomic fraction  $c$  of a second component in solid solution,  $d_r$  is the strain-free spacing of the pure (reference)

material and  $f(c)$  is some function of  $c$  that is known from theory or experiment. In the case where Vegard's law holds,  $f(c) = kc$  where  $k$  is a constant.

The presence of intrinsic stacking faults with a density  $\alpha'$  and of, possibly, extrinsic stacking faults with a density  $\alpha''$  causes a change in (apparent) lattice spacing according to

$$\frac{d_f - d_{nf}}{d_{nf}} = -\frac{3^{\frac{1}{2}}}{4\pi} C(hkl)(\alpha' - \alpha''), \quad (22)$$

where  $d_f$  and  $d_{nf}$  are the (strain-free) spacings of the material with and without faulting and  $C(hkl)$  is a parameter depending on  $h$ ,  $k$  and  $l$  (Wagner 1966; Warren 1969). Equation (22) only holds for spacings derived from peak maximum positions. For Cu and diluted Cu alloys, i.e. for fcc metals with stacking faults occurring on all  $\{111\}$  planes, the value of  $C(hkl)$  is known.

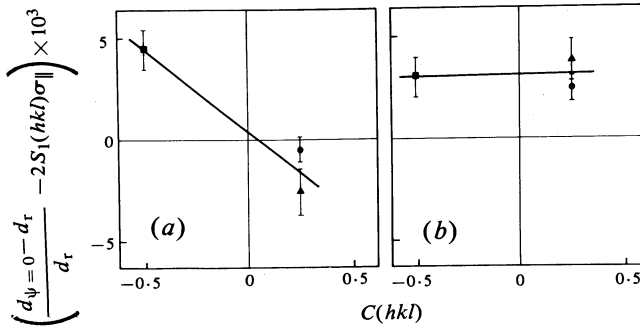


Fig. 4. Left-hand side of (23) versus  $C(hkl)$  for (a) an as evaporated and (b) a laser-irradiated CuCr multilayer on a Cu substrate. Data are for the reflections  $\{111\}$ , triangles;  $\{200\}$ , squares; and  $\{220\}$ , circles, of the Cu-rich phase.

Table 1. Data obtained from peak positions of the Cu-rich phase in a CuCr multilayer on a Cu substrate

Multilayer	Stress $\sigma_{\parallel}$ (MPa)	Stacking faults $\alpha' - \alpha''$	Composition $c$ of Cu-rich phase (at.% Cr)
As evaporated	155	$6 \times 10^{-2}$	$\approx 0$
Laser irradiated	935	$\approx 0$	4

From equations (20)–(22) it follows (to a high degree of accuracy) for the lattice spacing at  $\psi = 0$  of a stressed material with stacking faults and with a component in solid solution that

$$\frac{d(\psi=0) - d_r}{d_r} - 2S_1(hkl)\sigma_{\parallel} = -\frac{3^{\frac{1}{2}}}{4\pi} (\alpha' - \alpha'') C(hkl) + f(c). \quad (23)$$

For a number of reflections (with different  $hkl$  values for the left-hand side of (23) can be found experimentally. Then, from a plot of these values versus  $C(hkl)$ , the

values for  $\alpha' - \alpha''$  and  $f(c)$ , and thus  $c$ , are found from the slope and intercept of the straight line through the data points (see Fig. 4). The results for the CuCr layers are given in Table 1. To avoid serious errors,  $d(\psi=0)$  and  $d_T$  were measured on the same diffractometer and under the same conditions.

*(b) Peak Shape Analysis in Conjunction with Peak Position Analysis; Macro- and Microstrains near Welds*

Residual stresses near welds are highly complex in nature. They are caused by the thermal cycle accompanying the welding process. More specifically, they are believed to be due to non-uniform plastic deformation (for various reasons) of the material. By measuring both (macro)stresses from peak positions (cf. equation 18) and the amount of plastic deformation from line broadening (microstrain, cf. equations 1 and 14) simultaneously, a better insight can be gained on the origin of the stresses and also on the behaviour of the welded material in constructions (e.g. fatigue resistance behaviour).

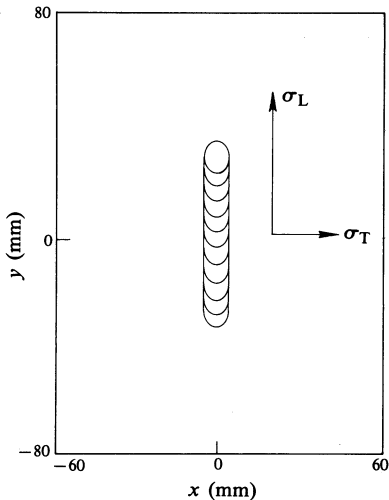


Fig. 5. Schematic drawing of a welded plate (thickness 4 mm), with definitions of coordinates and stresses as indicated.

Single pass bead-on-plate autogeneous TIG welds were made over about one-third of the length of a polished steel plate (see Fig. 5). Before welding, the plates were annealed to a stress level of about 10 MPa. The welding was carried out in an Ar-filled glove box.

On the basis of equation (18)  $\sigma_T$  and  $\sigma_L$  were determined as a function of  $x$  (see Fig. 6). Analysis of the microstrain was performed by means of the single-line Voigt method (see Section 3) for lattice planes parallel to the surface of the plate. The reference profile was taken from the welded plate under investigation, but at a position far away from the weld. So, relative determinations were made (cf. Section 3) and therefore only the effects of the welding process itself were studied. The integral breadths of the Cauchy component  $\beta_{C,m}^f$  were almost zero. In Fig. 7 the relative microstrain  $\tilde{\epsilon}_m$  is given as a function of  $x$ .

Since the steel plates were polished, it was possible to observe near the welds Lüders bands, which were due to plastic deformation occurring during the welding process. For the welded plate to which Figs 6 and 7 refer, the region with Lüders bands extended over a distance to the weld of  $x = 22$  mm. This is precisely the distance

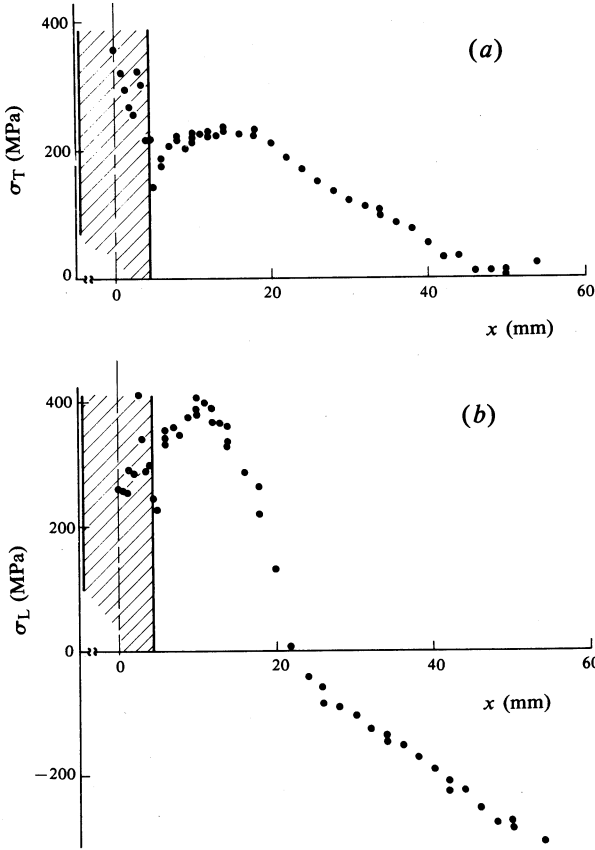


Fig. 6. Stresses (a)  $\sigma_T$  and (b)  $\sigma_L$  at  $y = 0$  in a TIG welded (150A) 4 mm thick steel plate as a function of distance  $x$  to the weld.

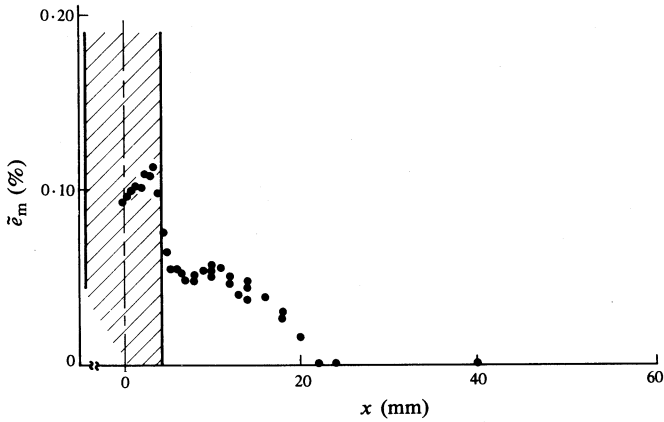


Fig. 7. Relative microstrain  $\tilde{\epsilon}_m$  at  $y = 0$  in a TIG welded (150A) 4 mm thick steel plate as a function of distance  $x$  to the weld.

at which the stress parallel to the weld  $\sigma_L$  changes from tensile to compressive (Fig. 6) and at which the relative microstrain  $\bar{\epsilon}_m$  reaches zero (Fig. 7)! Details about the experiments and their interpretations will be given in Brand *et al.* (1988).

In the practice of steel welding it is impossible to keep surfaces clean and to detect regions of plastic deformation optically. X-ray diffraction is not hindered seriously by (thin) surface layers due to contamination. The above shows that then quantitative information about plastic deformation can be obtained from the line broadening of the same profiles already measured for the sake of stress determination from peak positions. This can yield vital information at almost no extra cost.

## References

- Adler, T., and Houska, C. R. (1979). *J. Appl. Phys.* **50**, 3282–7.
- Bertaut, E. F. (1950). *Acta Crystallogr.* **3**, 14–8.
- Brand, P. C., Keijser, Th. H. de, Ouden, G. den, and Luyendijk, T. (1988). (To be published.)
- Cohen, J. B., Dölle, H., and James, H. R. (1980). In 'Accuracy in Powder Diffraction', NBS Spec. Publ. 567 (Eds S. Block and C. R. Hubbard), pp. 453–77 (NBS: Washington, D.C.).
- Delhez, R., Keijser, Th. H. de, and Mittemeijer, E. J. (1980). In 'Accuracy in Powder Diffraction', NBS Spec. Publ. 567 (Eds S. Block and C. R. Hubbard), pp. 213–53 (NBS: Washington, D.C.).
- Delhez, R., Keijser, Th. H. de, and Mittemeijer, E. J. (1982). *Fresenius Z. Anal. Chem.* **312**, 1–16.
- Delhez, R., Keijser, Th. H. de, Mittemeijer, E. J., and Langford, J. I. (1986). *J. Appl. Crystallogr.* **19**, 459–66.
- Delhez, R., and Mittemeijer, E. J. (1976). *J. Appl. Crystallogr.* **9**, 233–4.
- Hauk, V. M., and Macherauch, E. (1983). In 'Advances in X-ray Analysis', Vol. 27 (Eds J. B. Cohen *et al.*), pp. 81–99 (Plenum: New York).
- Keijser, Th. H. de, Langford, J. I., Mittemeijer, E. J., and Vogels, A. B. P. (1982). *J. Appl. Crystallogr.* **15**, 308–14.
- Keijser, Th. H. de, and Mittemeijer, E. J. (1978). *Z. Naturforsch.* **33a**, 316–20.
- Keijser, Th. H. de, and Mittemeijer, E. J. (1980). *J. Appl. Crystallogr.* **13**, 74–7.
- Klug, H. P., and Alexander, L. E. (1974). 'X-ray Diffraction Procedures for Polycrystalline and Amorphous Materials', 2nd edn (Wiley: New York).
- Langford, J. I., Delhez, R., Keijser, Th. H. de, and Mittemeijer, E. J. (1988). *Aust. J. Phys.* **41**, 173.
- Rothman, R. L., and Cohen, J. B. (1969). In 'Advances in X-ray Analysis', Vol. 12 (Eds C. S. Barret *et al.*), pp. 208–35 (Plenum: New York).
- Turunen, M. J. (1976). In 'Computer Simulation for Materials Applications' (Eds R. J. Arsenault *et al.*) *Nuclear Metallurgy* **20**, part 2, 850–7.
- Turunen, M. J., Keijser, Th. H. de, Delhez, R., and Pers, N. M. van der (1983). *J. Appl. Crystallogr.* **16**, 176–82.
- Wagner, C. N. J. (1966). In 'Local Atomic Arrangements Studied by X-ray Diffraction' (Eds J. B. Cohen and J. E. Hilliard), pp. 217–69 (Addison-Wesley: Reading, Mass.).
- Warren, B. E. (1969). 'X-ray Diffraction' (Addison-Wesley: Reading, Mass.).
- Warren, B. E., and Averbach, B. L. (1950). *J. Appl. Phys.* **21**, 595–9.
- Westendorp, J. F. M., Koelewijn, W., Sark, W. G. J. H. M. van, Saris, F. W., Pers, N. M. van der, and Keijser, Th. H. de (1986). *J. Mater. Res.* **1**, 652–60.
- Wilkens, M. (1979). *J. Appl. Crystallogr.* **12**, 119–25.
- Wilson, A. J. C. (1963). 'Mathematical Theory of X-ray Powder Diffractometry' (Philips Technical Library, Centrex: Eindhoven).
- Zemitis, M. A., Kidron, A., and Cohen, J. B. (1972). *Scripta Met.* **6**, 875–82.

